[3] G. Miano, L. Verolino, and V. G. Vaccaro, "A hybrid procedure to solve Hallén's problem," *IEEE Trans. Electromagn. Compat.*, vol. 38, no. 3, pp. 495–498, Aug. 1996.
[4] F. M. Tesche, M. V. Ianoz, and T. Karlsson, *EMC Analysis Methods and Computational Models*. New York, Wiley, 1997, ch. 4.
[5] B. Archambeault, O. M. Ramahi, and C. Brench, *EMI/EMC Computational Modeling Handbook*. Norwell, MA: Kluwer, 1998, ch. 4, 7.
[6] L. K. Warne and K. C. Chen, "Slot apertures having depth and losses described by local transmission line theory," *IEEE Trans. Electromagn. Compat.*, vol. 32, no. 3, pp. 185–196, Aug. 1990.
[7] D. Poljak, C. Y. Tham, and A. McCowen, "Transient response of nonlinearly loaded wires in a two media configuration," *IEEE Trans. Electromagn. Compat.*, vol. 46, no. 1, pp. 121–125, Feb. 2004.
[8] D. Poljak and V. Doric, "Time-domain modeling of electromagnetic field coupling to finite-length wires embedded in a dielectric half-space," *IEEE Trans. Electromagn. Compat.*, vol. 47, no. 2, pp. 247–253, May 2005.
[9] F. Gronwald, "Calculation of mutual antenna coupling within rectangular enclosures," *IEEE Trans. Electromagn. Compat.*, vol. 47, no. 4, pp. 1021–1025, Nov. 2005.
[10] C. A. Balanis, *Antenna Theory: Analysis and Design*, 3rd ed. New York: Wiley, 2005, sec. 8.3, 8.5.2.
[11] G. Fikioris, J. Lionas, and C. G. Lioutas, "The use of the frill generator in thin-wire integral equations," *IEEE Trans. Antennas Propag.*, vol. 51, no. 8, pp. 1847–1854, Aug. 2003.
[12] P. J. Davies, D. B. Duncan, and S. A. Funken, "Accurate and efficient algorithms for frequency domain scattering from thin wire," *J. Comput. Phys.*, vol. 168, pp. 155–183, 2001.
[13] D. H. Werner, "A method of moments approach for the efficient and accurate modeling of moderately thick cylindrical wire antennas," *IEEE Trans. Antennas Propag.*, vol. 46, no. 3, pp. 373–382, Mar. 1998.
[14] G. Fikioris, "An application of convergence acceleration methods," *IEEE Trans. Antennas Propag.*, vol. 47, no. 12, pp. 1758–1760, Dec. 1999.
[15] W. L. Stutzman and G. A. Thiele, *Antenna Theory and Design*. New York: Wiley, 1998.
[16] *NEC-WIN PRO User's Manual*, Antenna Analysis Software Version 1.1, Nittany Scientific, Inc., Hollister, CA, 1997.
[17] B. P. Rynne, "On the well-posedness of Pocklington's equation for a straight wire antenna and convergence of numerical solutions," *J. Electromagn. Waves Appl.*, vol. 14, pp. 1489–1503, 2000.
[18] M. C. van Beurden and A. G. Tijhuis, "Analysis and regularization of the thin-wire integral equation with reduced kernel," *IEEE Trans. Antennas Propag.*, vol. 55, no. 1, pp. 120–129, Jan. 2007.
[19] T. T. Wu, "Introduction to linear antennas," in *Antenna Theory, Part I*, R. E. Collin and F. J. Zucker, Eds. New York: McGraw-Hill, 1969, ch. 8, pp. 312–313.
[20] S. A. Schelkunoff, *Advanced Antenna Theory*. New York: Wiley, 1952, pp. 149–150.
[21] G. Fikioris and T. T. Wu, "On the application of numerical methods to Hallén's equation," *IEEE Trans. Antennas Propag.*, vol. 49, no. 3, pp. 383–392, Mar. 2001.
[22] G. Fikioris and A. Michalopoulou, "On the use of entire-domain basis functions in Hallen's integral equation with the approximate kernel," in *Proc. Mediterranean Microw. Symp. (MMS 2006)*, Genoa, Italy, Sep. 19–21, pp. 64–67.

Modeling Radiated Emissions Due to Power Bus Noise From Circuit Boards With Attached Cables

Haixin Ke, K. Morishita, Todd Hubing, N. Kobayashi, and T. Harada

***Abstract*—A two-step technique for modeling the radiation from circuit boards with attached cables is developed and applied to various board–cable structures. The technique divides a complex source geometry into two components. One component consists of differential-mode sources and the pieces of the structure that contribute to the differential-mode radiation. The other component consists of common-mode sources at cable attachment points and the parts of the structure that play a role in the radiation due to common-mode cable currents. The two component geometries are much easier to model than the complete structure. This modeling approach also provides the modeler with insight regarding the design parameters that most influence one type of radiation or the other.**

***Index Terms*—Balance, common-mode current, power bus noise, radiated emissions.**

I. Introduction

Printed circuit boards (PCBs) often have copper power and return (or *ground*) planes, and the return planes are usually connected to metallic objects such as cables or enclosures. For these types of structures, noise voltages between the power and return planes may induce significant common-mode currents on the attached metallic objects resulting in unacceptable radiated emissions. Although the *sources* of noise are normally on the board, the *antennas* are often the larger attached objects [1], [2]. It is often desirable to model the electromagnetic coupling between the noise on the board and the attached objects; however, this kind of modeling can present a significant challenge for full-wave numerical modeling techniques due to the small dimension of the board thickness and the relatively large dimensions of the attached cables and chassis.

One technique for simplifying this type of simulation [3] employs the equivalence theorem and replaces the plane pair with a magnetic current around the edges of the board. This technique works well for calculating the differential-mode radiation directly from the plane pair, but it is not an efficient method for determining the common-mode voltages that drive attached cables and enclosures.

Since it is the common-mode currents induced on the cables that are the primary concern, it can be advantageous to isolate the differential-mode sources and focus the modeling on just those aspects of the configuration that contribute to the common-mode currents. Techniques that use this approach are described in [4] and [5].

Recently, a two-step modeling technique was proposed that derives two simpler structures from the original PCB with cable/chassis attachments [6]. The first structure consists of the board's power and return planes with the attached cables and chassis removed. The second structure includes the cables and chassis, but eliminates the power plane and the dielectric substrate. The first structure is modeled to calculate the differential-mode voltage distribution between the power and return planes. The differential-mode voltages at discontinuities in the plane pair are then converted to equivalent sources and applied to the second

Manuscript received September 25, 2008; revised November 3, 2008. First published March 16, 2009; current version published May 15, 2009.

H. Ke and T. Hubing are with Clemson University, Clemson, SC 29634 USA (e-mail: hxkeucl@clemson.edu; hubing@clemson.edu).

K. Morishita, N. Kobayashi, and T. Harada are with NEC Corporation, Sagamihara 229-1198, Japan.

Color versions of one or more of the figures in this paper are available online at http://ieeexplore.ieee.org.

Digital Object Identifier 10.1109/TEMC.2008.2010947

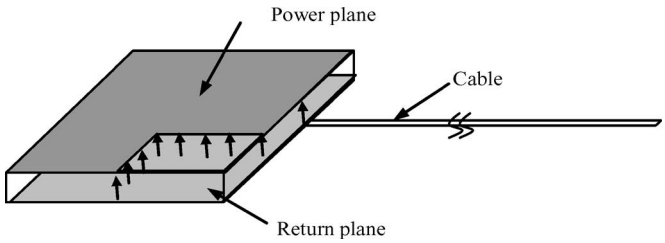

Fig. 1. Typical PCB structure.

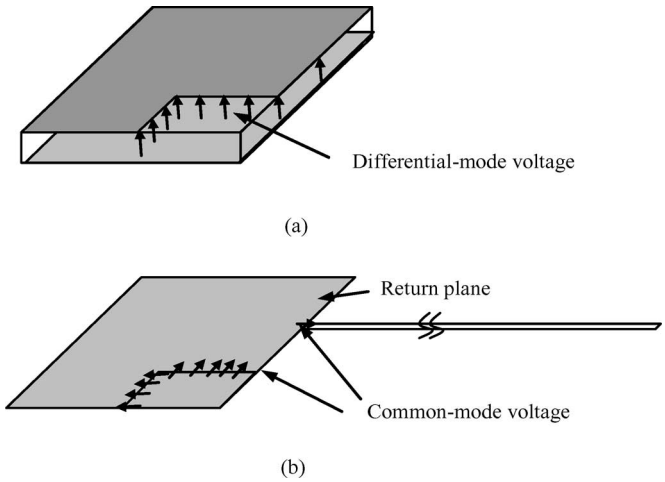

Fig. 2. Simpler structures of the two-step technique.

structure. The second structure can then be analyzed to determine the current distribution on the attached cables. Two simple examples were provided in [6]. However, the results presented in [6] do not validate the technique's ability to calculate far-field radiation, nor do they explore the range of applications for this technique. This paper refines and formalizes the two-step analysis procedure introduced in [6]. Several structures are analyzed that both validate and explore the limitations of this technique.

II. Description of the Technique

Fig. 1 illustrates a simple PCB structure consisting of a power and return plane separated by a dielectric substrate. A long cable is attached to one of the planes. Since the primary concern here is the common-mode current induced on the shield of the cable, the cable can be represented by a single conductor that is connected to the return plane of the board. Full-wave modeling of this structure is difficult due to the small scale of the plane separation combined with the large scale of the plane and cable.

Generally, the voltages between the planes are not significantly influenced by external objects attached to the board when the separation between the planes is small compared to the size of the planes. The first step of the two-step technique calls for the attached cable to be removed while the differential voltage distribution between the power and return planes is calculated. This can be done efficiently using cavity resonance models, circuit models, or 2-D or 3-D numerical models. Since we are interested in calculating common-mode currents, we can ignore the differential-mode voltages driving balanced parts of the structure. As shown in Fig. 2(a), it is the differential voltages at places where the plane edges do not coincide that are important. These are the only sources that affect the common-mode emissions.

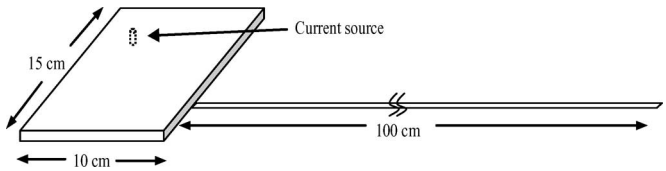

Fig. 3. PCB with one cable attachment.

In the second step, the cable is included, but the power plane and dielectric substrate are removed from the model. Delta-gap or magnetic frill voltage sources are placed in the return plane at every spot where the power and return planes did not coincide, as shown in Fig. 2(b). These are common-mode voltage sources and their value is one-half the value of the corresponding differential-mode voltage in the previous step. The factor of $\frac{1}{2}$ is due to the fact that the equivalent magnetic current sources associated with the common-mode voltages generate electromagnetic fields both above and below the planes, while the equivalent sources associated with the differential-mode voltages generate fields only above the planes. The equivalent structure in Fig. 2(b) is then analyzed using full-wave modeling techniques. The current distribution on the equivalent structure can be used to calculate the far-field radiation due to the common-mode current on the cable induced by power bus noise.

This two-step equivalent technique is much more efficient than a 3-D numerical method applied directly to the original structure. The number of elements required to accurately model the configuration in Fig. 2 is much smaller than that required to model the entire problem including the power plane. Boundary element method (BEM) techniques are particularly efficient for this application.

Consider the specific case of a PCB structure where the power and return planes have the same size. In this case, only one common-mode voltage source is necessary. This source is placed at the cable attachment point, which is the only place where the balance of the power planes is disrupted. Thus, the structure in the second step reveals the two halves of the antenna (i.e., the cable and the return plane) and the common-mode voltage source that drives this antenna. Moreover, the two-step model demonstrates that the amplitude of the common-mode current on the cable, and consequently the radiated emissions from the cable due to power bus noise, is determined by the voltage between the planes at the cable attachment point and is independent of the power bus noise anywhere else. This conclusion, which is not necessarily apparent from an examination of the full structure, becomes relatively clear and intuitive when the two-step modeling process is applied.

III. Numerical Results

To illustrate this technique, the simple PCB structure with one cable attachment shown in Fig. 3 is modeled. The board is 15 cm in length and 10 cm in width. It has solid power and return planes separated by a 0.2-cm dielectric substrate with a relative permittivity of $4.4-j0.066$. The board is excited by an ideal current source between the planes at a position 2.5 cm from the short side and 3 cm from the long side. A 1-m-long cable is attached to the longer side of the board 3 cm from the middle. The cable is modeled as a flat metal ribbon connected to the return plane. The width of the ribbon is 0.2 cm.

Fig. 4 shows the calculated current on the cable at the attachment point. The solid curve is the result obtained from a full-wave model of the entire configuration. A hybrid finite-element model (FEM)/BEM modeling technique [8] was employed in order to model the small-scale details of the fields between the planes and the larger scale currents on the cable simultaneously. The circles in Fig. 4 show the result obtained

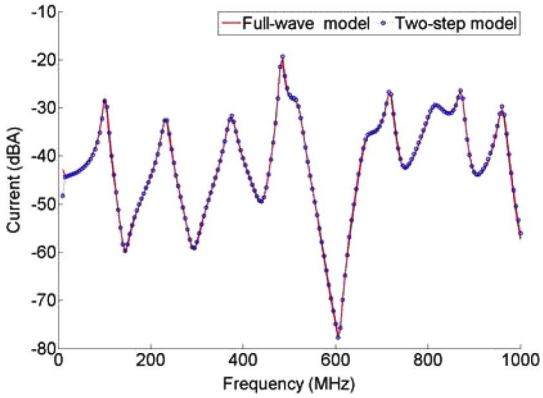

Fig. 4. Current on the cable of the one-cable example.

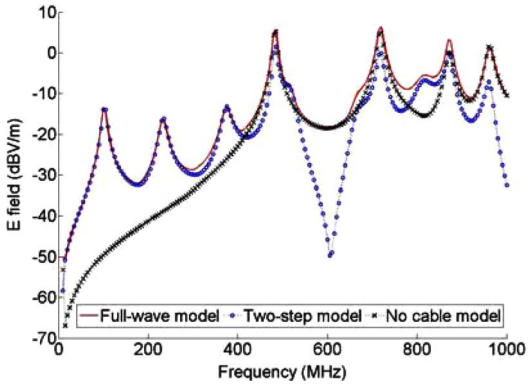

Fig. 5. 10-m far field for the one-cable example.

using the two-step equivalent method, which employed a cavity model to determine the fields between the planes and a relatively fast BEM simulation to determine the common-mode currents. The two curves agree very well from tens of megahertz to 1 GHz. In this example, the full-wave analysis employed 2134 tetrahedra and 1834 triangles, while the two-step BEM analysis required only 974 triangles and no tetrahedra.

Fig. 5 shows the radiated electric field magnitude 10 m from the source configuration. The maximum field occurring on the surface of a sphere with a 10-m radius was determined and plotted in the figure for each frequency. Again, the solid curve is the result obtained using the full-wave method while the circles show the results obtained with the two-step method. The crosses represent the maximum radiated E-field from the board with no cable.

It is easy to identify the radiation directly from the board and the radiation due to the cable in this figure. The figure shows that the two-step method results match the results of the full-wave model at cable resonances. At board resonances, the radiation due to the common-mode cable currents is several decibels lower than the radiation directly from the board. The sum (superposition) of the common-mode cable current radiation and the board-with-no-cable radiation is plotted in Fig. 6 and agrees well with the full-wave analysis of the complete system.

A similar PCB with two cables attached was also evaluated. Two cables are connected to the return plane on the long side of the board, as shown in Fig. 7. One cable has a length of 1 m and is 3 cm from the center. The other has a length of 60 cm and is 1 cm from the center. Both cables are flat ribbons with a width of 0.2 cm.

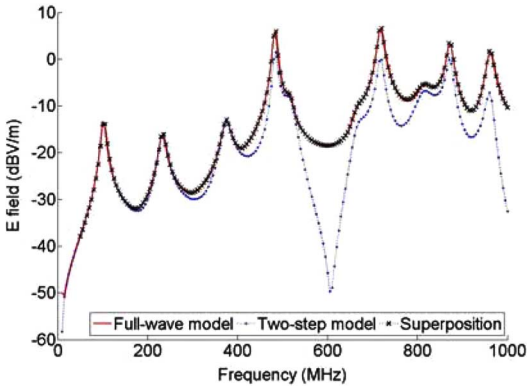

Fig. 6. Calculated far fields for the one-cable example.

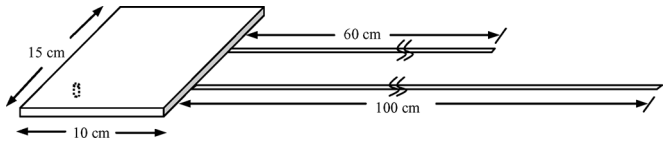

Fig. 7. Geometry of a two-cable PCB example.

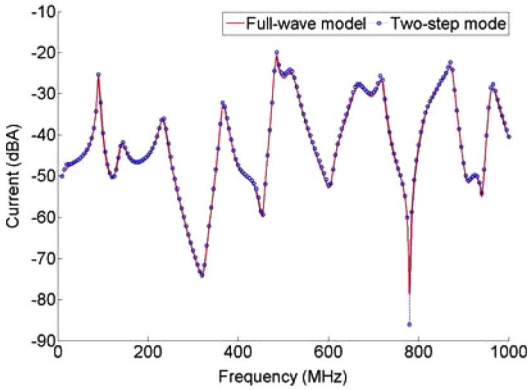

Fig. 8. Current on the longer cable in the two-cable example.

Fig. 8 shows the current at the connection point on the longer cable calculated using the full-wave model and the two-step method. The far-field results are plotted in Fig. 9. The two-step method did a good job of calculating the far field at the cable resonant frequencies. Also, the summed result of the equivalent model and emissions from the board with no cables matches the results obtained by a full-wave model of the original configuration.

Fig. 10 shows a geometry with a 5-cm cable connecting the PCB to a metal plate. The board has the same dimensions as the boards in the previous examples. The plate has the same length and width as the board.

The current on the cable near the connection to the PCB was calculated using the original full-wave and equivalent models. The results are plotted in Fig. 11. Fig. 12 compares the far fields calculated using the original model, the equivalent model, and the summation of the equivalent model results and the radiated emissions directly from the board with no cable. Again, the equivalent model does a good job of modeling the radiation due to the common-mode currents induced on the attached metal structure, while the differential-mode (i.e., no cable) model accurately determines the radiation directly from the board independent of the attached structures.

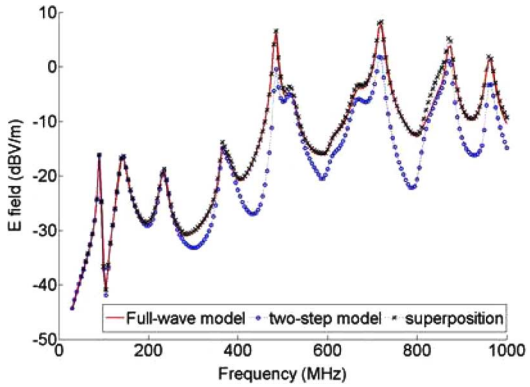

Fig. 9. Calculated far fields for the two-cable example.

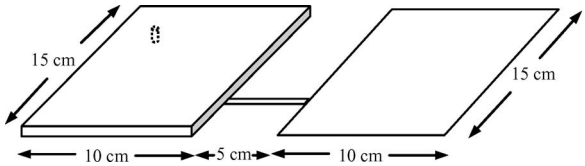

Fig. 10. Geometry of a PCB with plate attachment.

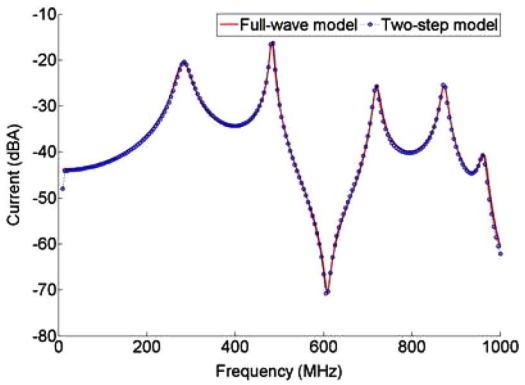

Fig. 11. Current on the short cable of the plate example.

Fig. 13 shows a similar board–cable configuration located near a finite ground plane. In this example, there is one cable attached to the long side of the board 3 cm from the center. The cable is a 1-m-long flat ribbon with a width of 0.2 cm. The 30 × 30 cm ground plane is located 2 cm below the board. The size of the plane is larger than that of the board. The plane introduces another source of imbalance allowing the differential-mode voltages at the PCB edges to couple energy to common-mode currents on the plate and cable.

The current on the cable was calculated and the results are shown in Fig. 14. The first three peaks are due to cable resonances. Note that the amplitudes of the second and third peaks calculated using the equivalent method differ from the full-wave results by several decibels. This indicates that the imbalance introduced by the ground plane allows differential-mode power bus noise around the perimeter of the board to affect the common-mode current induced on the cable.

Fig. 15 shows the far-field radiation results. In this example, the ground plane was included in the no-cable model when calculating the far field. Once again, the peaks at the second and third cable resonances exhibit several decibels of error.

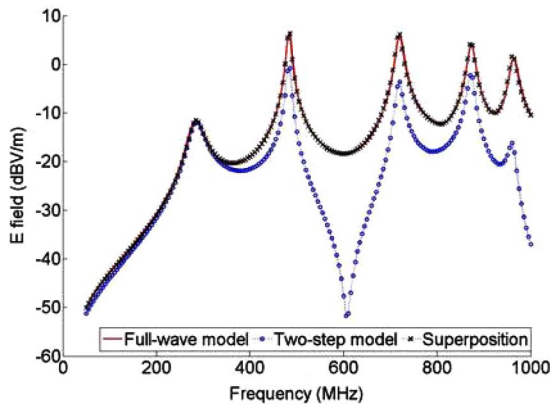

Fig. 12. Calculated far fields for the plate example.

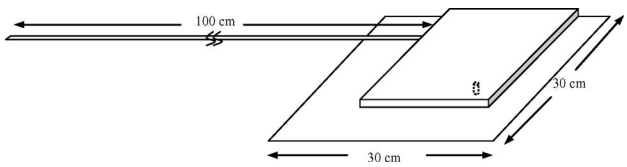

Fig. 13. Geometry of a PCB with cable and ground plane.

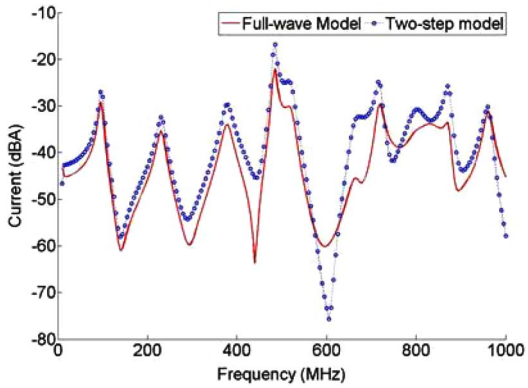

Fig. 14. Current on the cable of the ground plane example.

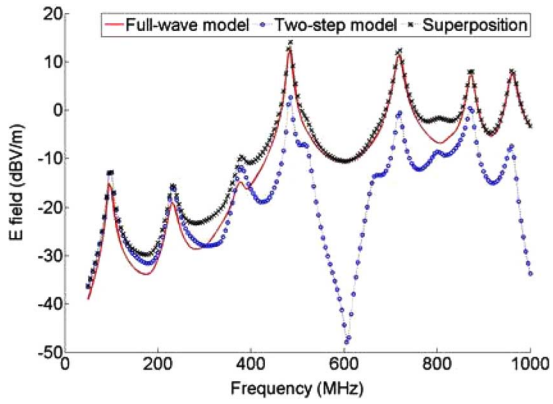

Fig. 15. Calculated far fields for the ground plane example.

IV. Conclusion

In this paper, typical PCB structures with metallic attachments were analyzed using a two-step modeling technique. Several examples

demonstrate how PCB structures can be modeled as the superposition of two simpler geometries: a balanced, differential-mode source geometry that neglects the attached structures and a common-mode source geometry that does not model the power plane or dielectric. Both current distribution and far-field radiation results are presented.

There was excellent agreement between the two-step approach and full-wave models of the entire configuration as long as the planes were well balanced. The common-mode noise sources appear only at places where there is an imbalance in the plane pair. However, a metal plate located 2 cm below the circuit board introduced sufficient imbalance to affect the common-mode coupling to an attached cable by several decibels.

The two-step modeling technique provides a simpler way to predict radiated emission from metallic attachments on circuit boards as long as all sources of imbalance are accounted for. It also provides the modeler with insight pertaining to the specific features of a source geometry that contribute most significantly to specific peaks in the radiated emissions by analyzing separately the contributions from differential-mode sources and common-mode sources.

REFERENCES

[1] T. H. Hubing and J. F. Kauffman, "Modeling the electromagnetic radiation from electrically small table top products," *IEEE Trans. Electromagn. Compat.*, vol. 31, no. 1, pp. 74–84, Feb. 1989.

[2] D. M. Hockanson, J. L. Drewniak, T. H. Hubing, T. P. Van Doren, F. Sha, and M. Wilhelm, "Investigation of fundamental EMI source mechanisms driving common mode radiation from printed circuit boards with attached cables," *IEEE Trans. Electromagn. Compat.*, vol. 38, no. 4, pp. 557–566, Nov. 1996.

[3] M. Leone, "The radiation of a rectangular power-bus structure at multiple cavity-mode resonances," *IEEE Trans. Electromagn. Compat.*, vol. 45, no. 3, pp. 486–492, Aug. 2003.

[4] K. B. Hardin and C. R. Paul, "Decomposition of radiating structures using the ideal structure extraction methods (ISEM)," *IEEE Trans. Electromagn. Compat.*, vol. 35, no. 2, pp. 264–273, May 1993.

[5] T. Watanabe, O. Wada, Y. Toyota, and R. Koga, "Estimation of common-mode EMI caused by a signal line in the vicinity of ground edge on a PCB," in *Proc. 2002 IEEE Int. Symp. Electromagn. Compat.*, Minneapolis, MN, Aug., pp. 113–118.

[6] K. Morishita, N. Kobayashi, T. Harada, H. Ke, and T. Hubing, "Modeling radiated emissions from cables attached to printed circuit boards driven by power bus noise," in *Proc. 2006 IEEE Int. Symp. Electromagn. Compat.*, Portland, OR, Aug., pp. 747–750.

[7] C. A. Balanis, *Antenna Theory*. New York: Wiley, 1996.

[8] Y. Ji and T. Hubing, "EMAP5: A 3D hybrid FEM/MOM code," *Appl. Comput. Electromagn. Soc. J.*, vol. 15, no. 1, pp. 1–12, Mar. 2000.

An Efficient Algorithm for Calculating the Earth Return Mutual Impedance of Conductors With Asymptotic Extraction Technology

Jun Zou, Jae Bok Lee, and Sug Hun Chang

***Abstract*—It is very essential to calculate the mutual impedance between overhead and buried conductors for analyzing electromagnetic compatibility problems related to a transmission line system. An efficient algorithm for calculating the Pollaczek integral, whose integrand oscillates rapidly and decays slowly, is proposed in this paper. With the help of the asymptotic extraction technique, the Pollaczek integral can be decomposed into the sum of two parts, one of which is expressed with an exponential integral and the other is the one that has a rapidly damped integrand. A comparison of the numerical results with published data shows very good agreement. The proposed approach is a good candidate for calculating impedances related to the Pollaczek integral.**

***Index Terms*—Asymptotic extraction technology, mutual impedance, Pollaczek integral.**

I. INTRODUCTION

The frequency-dependent earth return impedance between overhead and buried conductors is very essential for analyzing electromagnetic compatibility problems related to a transmission line system, for instance, power lines, cables, communication lines, gas pipes, etc. It is well known that the mutual impedance of interest here has been developed by Pollaczek in 1926 with a form of the so-called Pollaczek integral [1] that has been studied for decades due to its vital importance.

Generally speaking, algorithms for evaluating the Pollaczek integral can be classified into two categories. One is simplifying the Pollaczek integral to obtain a closed-form expression, for example, Lucca's formulation [2], the International Telegraph and Telephone Consultative Committee (CCITT) formulation [3], and Wedepohl and Wilcox's formulation [4]. For most of engineering applications, these formulations are accurate enough without needing time-consuming integrations. It is obvious that these aforementioned formulations can only be utilized under some specific conditions; the other is to calculate the Pollaczek's integral using a direct quadrature. The benefit of using numerical integration to evaluate the Pollaczek integral is that it can be applied with any parameter, say, different frequencies, arbitrary field points of interest, etc. The Pollaczek's integral is an inappropriate integral with a semiinfinite interval. Its upper limit must be truncated in practice, while a reasonable accuracy must be guaranteed. The integrand of the Pollaczek's integral is highly oscillatory when two conductors are well separated, and decays very slowly if two conductors are close to the surface of the earth. To expedite the integration calculation, a lot of research has been conducted in the past. Interested readers may refer to [5] that describes techniques to accelerate the calculation. The authors in [6] and [7] presented an elegant algorithm to calculate the earth return impedance between overhead and buried conductors. Although adopting an adaptive quadrature to evaluate the integral with a highly

Manuscript received August 6, 2008; revised November 29, 2008. First published April 14, 2009; current version published May 15, 2009. This work was supported by the National Natural Science Foundation of China under Grant. 50777038.

J. Zou is with the State Key Laboratory of Control and Simulation of Power Systems and Generation Equipments, Department of Electrical Engineering, Tsinghua University, Beijing 100084, China (e-mail: zoujun@tsinghua.edu.cn).

J. B. Lee and S. H. Chang are with the Electrical Environment Group, Korea Electrotechnology Research Institute, Changwon 641600, Korea.

Digital Object Identifier 10.1109/TEMC.2009.2016347